A HYDRAULIC (FLOW) UNIT BASED MODEL FOR THE DETERMINATION OF PETROPHYSICAL PROPERTIES FROM NMR RELAXATION MEASUREMENTS

Henry A. Ohen, Austin Ajufo and Federica Manni Curby, Core Laboratories, Houston.

ABSTRACT

This paper presents preliminary results of a Hydraulic Units (HU) based research program aimed at establishing guidelines for the use of nuclear magnetic resonance (NMR) tools for petrophysical evaluation. We show obvious but crucial relationships between the HU concept and NMR relaxation data which form the basis for linking NMR wireline log data to laboratory NMR measurements. Mathematical relationships between Flow Zone (hydraulic unit zonation) Indicators (FZI), specific surface area (S_{gv}), tortuosity (τ), surface relaxivity (ρ) and NMR longitudinal relaxation time T_1 are developed.

A permeability model based on FZI and NMR porosity is developed. Laboratory T_1 measurements at 1 MHz with CORESPEC-1000, together with core analysis data of permeability, porosity, centrifuge capillary pressure and thin section petrography have been used to validate the model. We also developed and validated HU-based predictive algorithms for estimating ρ and longitudinal relaxation time cut-off (T_{1c}) from pore throat size distributions (mercury injection data), and centrifuge capillary pressure data. We show that the observed variability in ρ is due to the existence of different hydraulic units in the reservoir rock. We also show that T_{1c} used for determining producible fluid from NMR relaxation time distributions may vary as a function of rock types.

INTRODUCTION

NMR logging tools have shown a very promising capability to determine permeability, producibility, non-producible water saturation, and residual oil saturation more accurately with less interpretational difficulties than conventional logging tools, but requires proper calibration to laboratory core data.

Development and successful application of HU technology for predicting petrophysical properties from wireline logs has been reported previously[1,2,3,4,5]. The HU concept combines geological (texture and mineralogy) and petrophysical (porosity, permeability and capillary pressure) controls of reservoir quality for the identification and delineation of reservoir rocks into units of similar fluid flow characteristics. The linkage between NMR and HU technologies is possible because T_1 and FZI are both related to the rock surface phenomenon which controls its microscopic attributes. Hence FZI forms the missing link required to utilize NMR logging for petrophysical data acquisition. We used T_1 data as a basis for developing our models for the purpose of validation with existing models[7,8] based on it. But T_2 data may be used since its relationship with T_1 has been established[9].

FUNDAMENTAL CONCEPT AND MODEL EQUATIONS

The concept of NMR and application of NMR relaxation data to reservoir rocks have been reported[7,8,9,10,11,14]. The multi-exponential model describing the magnetization decay, M(t) as a function given as follows;

$$\frac{M(t)}{M_0} = \sum_i A_i e^{-\frac{t}{T_i}} \quad \text{----------(1)}$$

where, A_i, the spectral amplitude, is the fraction of the total pore space containing fluid with a relaxation constant equal to T_i; and, t - time from start of application of the pulse.

Fundamental Equations

The apparent relaxation rate for a single pore in the porous media (assuming fast diffusion limit) is given as:

$$\frac{1}{T_1} = \frac{1}{T_b} + \rho F_{sv} \quad \text{---------- ---------(2)}$$

where, F_{SV} (μm^{-1}) is surface area to volume ratio of the pore space, and T_b and T_1 (sec) are the relaxation times for the bulk fluid and for the fluid in the porous medium, respectively. ρ, (μm/sec) - the surface relaxivity is influenced by surface composition (paramagnetic ions and absorbed compounds etc.). $T_b >> T_1$, hence

$$\frac{1}{T_1} = \rho F_{sv} \quad \text{----------(3)}$$

It has been shown[3] that:

$$F_{SV} = \frac{S_{gv}(1-\phi)}{\phi} \quad \text{----------} \quad \text{-(4)}$$

where, ϕ is the rock porosity, and S_{gv} - the specific surface area. Eq. 3 can be written as:

$$\rho T_1 = \frac{\phi}{S_{gv}(1-\phi)} \quad \text{---------- (5)}$$

Kozeny[12] and Carman[13] developed the following model for determining permeability from porosity:

$$K = \frac{1}{\tau^2 S_{gv}^2 F_s} \frac{\phi^3}{(1-\phi)^2} \quad \text{----------(6)}$$

where F_s is the shape factor of the porous medium. Unsuccessful attempts to compute permeability, K, from Eq. 6 using $\frac{1}{\tau S_{gv}\sqrt{F_s}}$ as a constant is attributable to the variability of this term as has been demonstrated by Amaefule et al[1]. who termed it the FZI, i.e.,

$$FZI = \frac{1}{\tau S_{gv}\sqrt{F_s}} \quad \text{----------(7)}$$

Combining Eqs. 6 and 7 gives the following in μm;

$$0.0314\sqrt{\frac{K}{\phi}} = FZI \frac{\phi}{1-\phi} \quad \text{----------(8)}$$

Amaefule et al.[1] call the term, $0.0314\sqrt{(k/\phi)}$ in Eq. 8, reservoir quality index (RQI) and employed it for hydraulic units zonation[1,2,4]. The combination of Eq. 5 and 8, therefore, forms the basis for relating T_1 to RQI, and hence hydraulic flow units, as follows:

$$RQI = 0.0314\sqrt{\frac{K}{\phi}} = \frac{\rho T_1}{\tau\sqrt{F_s}} \quad \text{----------(9)}$$

Eq. 9 suggests that RQI is related to relaxation time in the same way it is related to porosity group ($\Phi_z = \phi/(1-\phi)$) in the Amaefule et al. model[1]. Re-writing Eq. 5 and taking the logarithm of both sides of the resulting equation, we have as follows:

$$\log T_1 = \log \Phi_z + \log\left(\frac{1}{\rho S_{gv}}\right) \text{----------(10)}$$

Defining $C = \rho S_g$ in Eq. 10 and using the limited data presented in this work, we have demonstrated in Figure 4 that a plot of log T_1 versus the porosity group Φ_z should give a unit slope with a constant intercept equal to 1/C.

The Concept of HU Based on Core Permeability and Porosity

The hydraulic units concept is based on the fact that the FZI term in Eq. 8 is only constant within a certain volume of the reservoir that has similar fluid flow characteristics. Therefore, when the log of both sides of Eq. 8 is taken, we have:

$$\log (RQI) = \log (FZI) + \text{Log}(\Phi_z) \text{---------- (11)}$$

From Eq. 11, it is easy to see that if a log-log plot of RQI versus Φ_z is made, all data points that exhibit similar fluid flow characteristics will lie on the same unit slope line.

The Concept of HU Based on NMR Relaxation Data

In order to relate NMR to HU concept, we define FZIP (μm), which is similar to FZI as:

$$FZIP = \frac{\rho}{\tau\sqrt{F_s}} \quad \text{----------(12)}$$

Therefore, from Eq. 9 we obtain the following relationship between RQI and T_1

$$\log (RQI) = \log (FZIP) + \log T_1 \text{----------(13)}$$

From the definition of the reciprocal intercept, C, we obtain the relaxivity as a function Sgv as $\rho = C/S_{gv}$. Therefore, FZIP can be related to FZI as follows:

$$FZIP = \frac{C}{\tau S_{gv}\sqrt{F_s}} = C(FZI) \quad \text{----------(14)}$$

Eq. 14 indicates that like the hydraulic unit model[1], FZIP is a function of τ and S_{gv}, and hence, varies with mineralogy and textural properties which define rock types. This implies that the relationship between RQI and T_1 varies from one rock type or hydraulic flow unit to another. Like the log-log plot of RQI versus $\phi/(1-\phi)$ in the HU concept (Eq. 11, log-log of RQI versus T_1 (Eq. 13) yields a unit slope line for specific hydraulic units.

Pore and Pore Throat Sizes Distributions and Permeability

Pore size distribution is obtained from NMR T_1 using ρ. Some authors[8] have used constant values of ρ (ranging from 0.001 cm/sec to 0.007 cm/sec). We demonstrate below that ρ is a function of FZIP.

The mean hydraulic radius ($r_{rm} = r/2$) for a circular cylindrical pore throat with radius r is related to the surface area per unit grain volume (Sgv) and porosity (ϕ) as follows:

$$S_{gv} = \frac{2}{r}\frac{\phi}{1-\phi} \quad \text{----------(15)}$$

Therefore, FZI is given as:

$$FZI = \frac{1}{\tau\sqrt{F_s}}\frac{r_{rm}}{\Phi_z} \quad \text{---------- -----(16)}$$

It has been shown[1] that a plot of r_{mh}/Φ_z versus FZI yields a straight line with a slope equal to $\tau\sqrt{F_s}$. Data used in this study also confirm this observation. Re-writing Eq. 12, ρ is related to the hydraulic units characteristics variable, FZIP, as:

$$\rho = FZIP\,\tau\sqrt{F_s} \quad \text{----------(17)}$$

To accurately determine pore throat size distribution from NMR data, it is important to recognize the variability of the pore size to pore throat size ratios from one flow unit to another. Consider a simple spherical pore body with radius r_p such that:

$$F_{sv} = \frac{3}{r_p} \quad \text{---------- (18)}$$

From Eq. 3,

$$T_1 = \frac{r_p}{3\rho} \quad \text{---------- (19)}$$

Defining pore size to pore throat size ratio as $R_{pt} = r_p/r_t$, Eq. 19 can be written as;

$$T_1 = \frac{R_{pt}}{3\rho} r_t \quad \text{----------(20)}$$

A relationship which identifies hydraulic unit boundaries can be obtained by rearranging and taking the logarithm of both sides of Eq. 20:

$$\log(r_t) = \log(T_1) + \log\left(\frac{3\rho}{R_{pt}}\right) \quad \text{----------(21)}$$

Permeability Prediction

Permeability, K, depends on pore throat size but NMR measures pore size. Difficulty in predicting K from NMR data arises where there is a large variation in pore throat size to pore size ratio, as is often the case in carbonates where micro geometry is much more diverse than in clastics. K has typically been related to T_1 empirically in the form:

$$K = \Gamma\phi^a T_1^b \quad \text{----------(22)}$$

Amaefule et al.[1] relates K to porosity through FZI:

$$K = 1014\,(FZI)^2\,\phi^3 / (1-\phi)^2 \quad \text{----------(23a)}$$

They[1] also show the following non-linear relationship between FZI and S_{wir}.

$$S_{wir} = 1.0 - 1/(a+bFZI^{-c}) \quad \text{---------- (23b)}$$

In most clastics, the non-movable water saturation measured with correct core calibrated T_{1c} $NMRS_{WR}$ is equivalent to the rock irreducible water saturation S_{wir}. Hence, for predicting K with Eq. 23a-b in this work, we relate FZI to $NMRS_{WR}$ as follows:

$$FZI = (b(1.0- NMRS_{WR}))/(1.0+a(NMRS_{WR} -1))^{1/C} \quad \text{--------(23c)}$$

where, a, b and c are obtained by a non-linear regression on the database, and calibrated for a specific reservoir or field.

Movable and Capillary Bound Water

One of the uses of the NMR data is the determination of capillary bound water and movable fluid. The major issue in the estimation of these properties is the determination of the value of T_1 below which the surface to volume ratios of the porous media are too high for the fluid to be producible (T_{1c}). We believe this critical value is related to the flow zone indicator and therefore is a unique property of the flow units. As shown by Kenyon et al.[14], the capillary bound water is dependent on pore throat size which determines the critical pore throat size allowable for the primary drainage entry of the non-wetting phase. This critical pore throat radius r_{tc} is related to NMR data through R_{pt}. The following Young-Laplace equation is typically used to determine the r_{tc} based on capillary pressure:

$$r_{tc} = \frac{0.29\sigma \cos\theta}{p_c} \quad \text{----------(24)}$$

The corresponding T_{1c} is given as a function of R_{pt}, ρ, wettability and capillary pressure p_c as follows:

$$T_{1c} = \frac{R_{pt}}{3\rho}\frac{0.29\sigma \cos\theta}{p_c} \quad \text{----------(25)}$$

Eq. 25 indicates that T_{1c} is directly proportional to R_{pt} and inversely proportional to relaxivity while both ρ and R_{pt} vary as a function of HU. The question is, do the effects cancel out or does T_{1c} vary in a heteregenous rock system?. We find as shown in Table 1(a), that T_{1c} appears to be fairly constant within the data set we investigated. Integration of the decay time population density curves (Figures 1 and 2) from zero to T_{1c} gives the fraction of the pore space that is occupied by non-movable fluid, $NMRS_{WR}$, as follows:

$$NMRS_{WR} = \int_0^{T_{1c}} A(T_1)dT_1 \approx \sum_0^{T_{1c}} A(T_1) \text{--------(26)}$$

PRESENTATION AND DISCUSSIONS OF RESULTS

Results of the multi-exponential analysis[15] of the NMR T_1 relaxation measurements and computation of petrophysical data are presented for seventeen samples. The 1" long by 1" diameter core plugs used for this work were randomly selected from different reservoir rocks. The samples were 100% saturated with brine for the NMR measurements. Figures 1 and 2 are the T_1 distributions derived from the NMR inversion recovery data for Samples 1 and 7, respectively. The noise level is low enough to enable the existence of bimodal pore sizes to be recognized as can be seen in Figure 1.

Porosity and Relationship to NMR T_1

Table 1 shows porosity data acquired using the CMS-300 at 800 psi and the NMR-derived porosity of the core samples. A cross plot of the two sets of porosity data, shown Figure 3, show a near perfect match. We chose to plot log Φ_z versus log median T_1 as shown in Figure 4, but other T_1 data can be used. The unit slope line fitted to the data points gives an intercept of 0.4 at Φ_z =1.0 and confirms the theoretical basis of Eq. 10.

HU Zonation

Figures 5 and 6 compare the hydraulic units delineation using Amaefule et al.[1] and our NMR technique presented herein. Apart from one sample (ID # 6), the two methods separated the samples into four hydraulic units containing the same sample groups. This is a validation of the theoretical basis of the technique presented herein. Figure 7 is a plot of r_{mh}/Φ_z (mercury injection capillary pressure data) versus FZI which gives a unique slope equal to $\tau\sqrt{F_s}$ confirming the Amaefule et al[1]. observation. A value of 2.5 obtained for our data set with FZIPs obtained from Figure 6 is used to compute the surface relaxivity, ρ values for the different hydraulic units using Eq. 17. As shown in Table 1a, ρ varies from 0.005 μm/sec for the worst HU to 0.054 μm /sec for the best HU.

Pore/Throat Size Distribution

In order to convert NMR pore size to pore throat size, pore size to throat size ratios must be determined for each HU. The intercept at T_1=1.0 in Figure 8 gives $\gamma = R_{pt}/3\rho$ from which R_{pt} values are obtained as shown in Table 1. Figures 9 through 12 compare the pore throat sizes derived from NMR and mercury injection data. The match is reasonably good considering that the distributions from mercury injection are obtained by finite difference approximation applied to the mercury saturation and not therefore expected to be a smooth function.

Movable and Capillary Bound Water

The 100% saturated samples were desaturated by centrifuging up to 400 psi capillary pressure. Variations in T_{1c} at 50 psi and 400 psi were insignificant. Median/mode values of 20 ms at 50 psi and 10 ms at 400 psi were obtained from the statistical analysis of 11 samples (Table 1b). Figures 13 and 14 show that water saturation obtained with T_{1c} = 10 ms (calibrated to 400 psi centrifuge capillary pressure) follows the same trend as the established relationship between S_{wir} and FZI. Figure 14 also shows that water saturation obtained by centrifuging to 50 psi (equivalent T_{1c} = 20 ms) may be movable.

NMR Permeability

To predict permeability shown Table 1a from NMR porosity and FZI using Eq. 23a, FZI was determined with Eq. 23c. Figure 15 shows the result of the non-linear regression between FZI and $NMRS_{WR}$ in which a = 0.995, b = 0.3 and c = 0.508 are used in Eq. 23c to determine FZI. Figure 16 is a near perfect match (within the database used for the regression) between measured permeability and permeability determined by this model.

Petrographic Interpretation of the NMR data

Examples of thin section descriptions are presented to explain the results of the multi-exponential analysis of the NMR relaxation data. Samples 1,2,7 and 10 were selected as examples from HU 1,2,3 and 4 respectively. As shown in Figure 17, there is reasonable similarity between the mercury injection pore throat size and NMR pore size distributions. The petrographic description of the pore scale observations is as follows:

Sample 1 -HU 3: The microporosity resulting in the bimodal pore-size distribution in this sandstone is due to the presence of moderately common authigenic, pore-filling kaolinite and scattered, partially dissolved feldspars and rock fragments. Macropores occur as intergranular pores and dissolution pores. The bimodal pore size distribution is accentuated by the variability in grain size.

Sample 2 - HU 1: The uniform grain size and generally, clay-free nature of this sandstone has resulted in a very uniform macroporous network. The small amount of microporosity present is due to scattered, partially dissolved rock fragments.

Sample 7 - HU 4: The only pores visible in this limestone are intercrystalline pores associated with the sparry calcite cement. The fracture visible in this view is artificial and an artifact of sampling. No micropores are observed.

Sample 10 - HU 2: Most pores in this sandstone are macropores which occur as intergranular pores or dissolution pores. The small amount of microporosity present is due to small, scattered patches of kaolinite, and a few partially dissolved rock fragments.

CONCLUSIONS

- NMR relaxation measurements can be used to sort rock samples into Hydraulic Units.
- It appears that T_{1c} is independent of HU, but may be as low as 10 ms in order to determine the true irreducible (non centrifugable) water saturation
- NMR relaxation information, when calibrated to core analysis data, is a very useful tool for determining porosity and for estimating permeability. In an air-water system, Free Fluid Index (FFI) and Bulk Volume Irreducible (BVI) water was determined.
- Relative abundance of micro to macro porosity can be inferred from NMR T_1 distributions obtained using the multi-exponential model.

RECOMMENDATIONS

Reservoir or field specific calibration to core analysis data is required to obtain reasonable values for ρ, T_{1c} and the FZI - $NMRS_{WR}$ relationship for effective utilization of NMRL data.

ACKNOWLEDGMENTS

The authors thank Core Laboratories for the permission granted to publish this manuscript. Additional thanks is due to Joe Weir, Don Harville and Jerry Warne for performing the laboratory tests and measurements.

REFERENCES

1. Amaefule, J.O. et al."Enhanced Reservoir Description: Using Core and Log Data to Identify Hydraulic (Flow) Units and Predict Permeability in Uncored Intervals/Wells", SPE 26436, 68th Annual SPE conference and exhibition, Houston, Texas, October 3rd - 6th, 1993.
2. Amaefule, J. O, Altunbay M, Henry Ohen, Kersey David and Lane Peter "A Hydraulic (Flow) Units-Based Approach for Predicting Formation Damage in Uncored interval/ Wells using core/log data.," Presented at the International Symposium on Formation Damage Control, 9-10 February, 1994.
3. Geogi, D. T. and Menger, S.K: "Reservoir Quality, Porosity and Permeability Relationships," Paper presented at the Mintrop Seminar Germany, May, 1994.
4. Ohen Abuya Henry, Nnabuihe Larry and Ososanwo Dunni: "Laboratory Acid Effectiveness Evaluation is the Key to Productivity Improvement by Acidizing in the Clayey Agbada Formation of the Niger Delta," paper SPE 30101, presented at the SPE European Formation Damage Conference held in Hague, Netherlands, May 15-16, 1995.
5. Hassan Bin Tajul Amar, Altunbay Mehmet and Bar Duncan: " Stress Sensitivity in the Dulang Field - How it is Related to Productivity ," paper SPE 30092, presented at the SPE European Formation Damage Conference held in Hague, Netherlands, May 15-16, 1995.
6. Udegbunam E.O., and Huff B.G : "Geological Characterization and 3-D Visualization of the Gas Storage Reservoir at Hillsboro Field, Montgomery County, IL," Paper SPE 29158, presented at the 1994 Eastern Regional meeting in Charleston WV, 8-10 November, 1994.
7. Kenyon, W.E, Day, P.I., Straley, C., and Willemson, J.F.,: "A three-part study of NMR longitudinal relaxation properties of water saturated sandstones," SPE Formation Evaluation, p 622-36, Sept. (1988).
8. Kenyon, W.E., Howard, J.J, Sezginer, A. Straley, C., Matteson, A., Horkowitz, K. and Ehrlich, R. : " Pore-sized distribution and NMR microporous cherty sandstones," Trans., 30th Annual SPWLA Symposium, paper LL, June ,1989
9. Straley, C. Morriss, C.E. Kenyon, W.E., and Howard, J.J.,: "NMR in partially saturated rocks: laboratory insights on free fluid index and comparison with borehole logs, " Trans., 32nd Annual SPWLA Symposium, paper CC, June, 1991.
10. Dunn K.J., Latorraca, G.A., Warner, J.L., and Bergman, D.J.,: "On the Calculation and Interpretation of NMR Relaxation Time Distributions", paper SPE 28367, presented at the 1994 Annual Conference and Exhibition in New Orleans, Sept. 25-28.
11. Morriss C.E., et al. : "Field Test of an Experimental Pulsed Nuclear Magnetism Tool," SPWLA 34th Logging Symposium, June 13-16, 1993.
12. Kozeny, J. : "Uber Kapillare Leitung des Wassers im Boden, Sitzungsberichte, " Royal Academy od Science, Vienna, Proc. Class I(1927) v. 136, 271-306.
13. Carman, P.C. : Fluid Flow through granular Beds, " Trans. AICHE (1937) v 15, 150-166.
14. Kenyon W.E. et al.: "A Laboratory Study of Nuclear Magnetic Resonance Relaxation and its Relation to Depositional Textural and Petrophysical Properties - Carbonate Thamama Group, Mubarraz Field, Abu Dhabi, " paper SPE 29886, presented at the SPE Middle East Oil Show held in Bahrain, 11-14 March, 1995.
15. Kenyon W.E et al : "Compact and Consistent representation of Rock NMR data for Permeability Estimation." SPE 15643.

Table 1a: Core Analysis and Core NMR Data

Sample I.D. #	CMS-300 Porosity Fraction	NMR Porosity Fraction	CMS-300 Perm. mD	NMR Perm. mD	Median T_1 sec	RQI μm	FZI Core μm	FZI Calcu. μm	FZIP μm	HU #	T_{1C} 50 psi ms	T_{1C} 400 psi ms	ρ_{ave} μm/ms	Throat Size μm	γ μm	R_{pt}	S_{WIR} (Centrif %)	$NMRS_{WR}$ (50psi) %	$NMRS_{WR}$ (400 psi) %
2	0.255	0.264	1760.0	2003.4	0.121	2.609	7.621	10.254	21.51	1	15.0	10.0	0.0538	10.00	120	1.344	9.6	18.0	8.0
6	0.184	0.179	794.0	717.0	0.302	2.063	9.148	10.254	6.83	1	20.0	10.0	0.0538	18.00	120	1.345	7.6	12.0	8.0
5	0.232	0.232	240.0	240.4	0.126	1.010	3.343	6.479	8.02	2	18.0	10.0	0.0245	4.80	50	1.470	6.7	20.0	10.0
9	0.263	0.265	778.0	801.6	0.106	1.708	4.786	6.479	16.11	2	15.0	8.0	0.0245	8.50	50	1.470	2.7	17.0	10.0
10	0.136	0.160	31.9	54.9	0.086	0.481	3.055	1.769	5.62	2			0.0245	2.00	50	1.470	18	25.0	18.0
14	0.226	0.251	164.0	241.5	0.095	0.846	2.897	4.398	8.89	2			0.0245	5.00	50	1.470		18.0	12.0
18	0.155	0.160	74.9	82.5	0.074	0.690	3.763	2.021	9.29	2	19.5	10.0	0.0245	3.00	50	1.470	16	25.0	17.0
19	0.222	0.234	400.0	481.1	0.122	1.333	4.671	2.324	10.93	2	15.0	10.0	0.0245	7.50	50	1.470	9.8	20.0	16.0
16	0.228	0.254	98.0	145.2	0.098	0.651	2.204	3.139	6.64	2			0.0245	4.50	50	1.470		20.0	14.0
1	0.194	0.197	48.0	50.2	0.064	0.494	2.052	1.557	7.74	3	20.0	9.5	0.0150	1.00	25	1.800	7.8	28.0	19.0
4	0.166	0.141	16.1	9.4	0.071	0.309	1.554	1.769	4.34	3			0.0150	0.40	25	1.800		27.0	18.0
13	0.206	0.224	65.5	87.6	0.088	0.560	2.158	2.324	6.33	3			0.0150	1.00	25	1.800		24.0	16.0
17	0.145	0.147	9.2	9.6	0.058	0.250	1.472	1.557	4.31	3	20.0	9.5	0.0150	0.60	25	1.800	11.5	28.0	19.0
3	0.091	0.102	0.2	0.2	0.028	0.043	0.432	0.310	1.57	4	20.0	10.0	0.0048	0.18	7	2.057	34.7	45.0	35.0
7	0.058	0.060	0.0	0.0	0.027	0.027	0.434	0.713	0.99	4			0.0048	0.30	7	2.036		40.0	26.0
11	0.121	0.113	0.9	0.7	0.031	0.086	0.623	0.404	2.77	4	20.0	10.0	0.0048	0.35	7	2.036	25.9	40.0	32.0
15	0.145	0.132	2.8	2.1	0.066	0.138	0.812	0.976	2.09	4	20.0	10.0	0.0048	0.60	7	2.036	18	30.0	23.0

Table 1b: Descriptive Statistics & Results of Regression Analysis

		FZI μm		FZIP μm		T_{1C} @ (50psi)	T_{1C} @ (400psi)
HU	4	3	4	3	2.00		
Mean	0.575	1.888	1.855	5.873	9.81	18.41	9.73
SE	0.091	0.156	0.377	0.674	1.45	0.68	0.18
Median	0.528	2.052	1.831	6.334	9.09	20.00	10.00
Mode	#N/A	#N/A	#N/A	#N/A	#N/A	20.00	10.00
SD	0.181	0.348	0.754	1.508	3.54	2.27	0.61
SV	0.033	0.121	0.568	2.274	12.56	5.14	0.37
Kurtosis	-1.294	-3.022	-0.610	-2.171	2.16	-1.08	7.94
Skewness	0.854	-0.529	0.164	-0.044	1.16	-0.98	-2.74
Range	0.380	0.732	1.772	3.436	10.49	5.00	2.00
Minimum	0.432	1.472	0.993	4.305	5.62	15.00	8.00
Maximum	0.812	2.204	2.766	7.742	16.11	20.00	10.00
Sum	2.301	9.440	7.420	29.367	58.86	202.50	107.00
Count	4	5	4.000	5	6.00	11.00	11.00

1995 SCA Conference Paper Number 9514

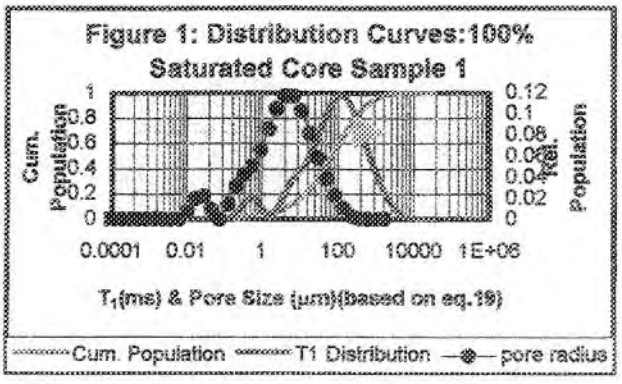
Figure 1: Distribution Curves:100% Saturated Core Sample 1
Cum. Population
Rel. Population
0.0001 0.01 1 100 10000 1E+06
T1(ms) & Pore Size (µm)(based on eq.19)
Cum. Population
T1 Distribution
pore radius

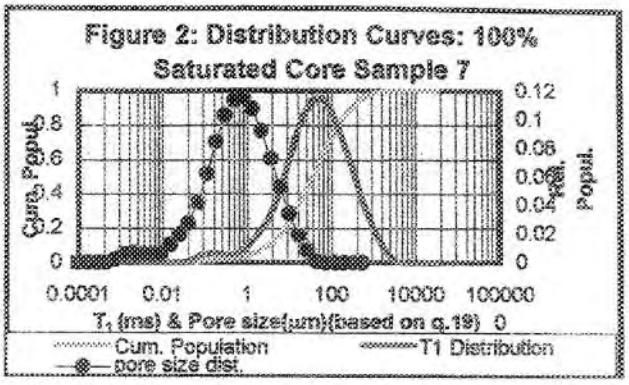
Figure 2: Distribution Curves: 100% Saturated Core Sample 7
Cum. Popul.
Rel. Popul.
0.0001 0.01 1 100 10000 100000
T1 (ms) & Pore size(µm)(based on q.19) 0
Cum. Population
T1 Distribution
pore size dist.

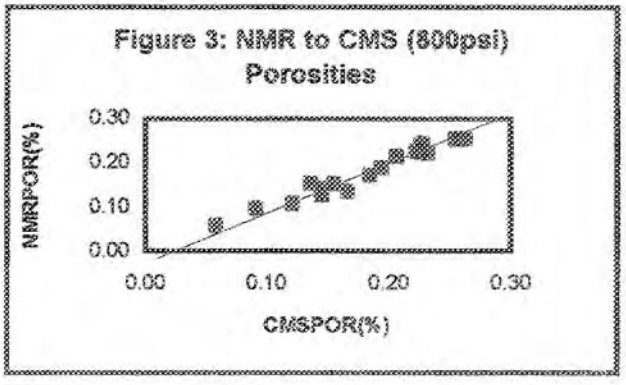
Figure 3: NMR to CMS (800psi) Porosities
NMRPOR(%)
CMSPOR(%)

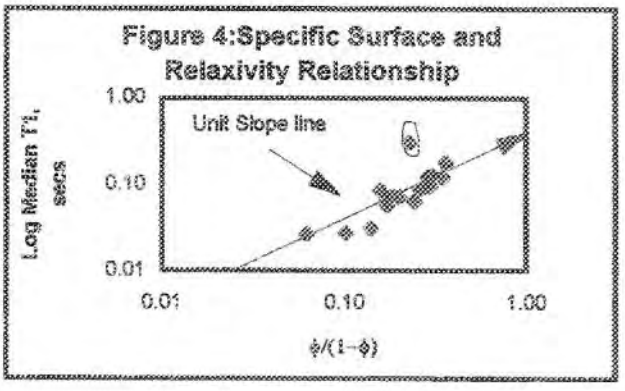
Figure 4:Specific Surface and Relaxivity Relationship
Log Median T1, secs
Unit Slope line
ϕ/(1−ϕ)

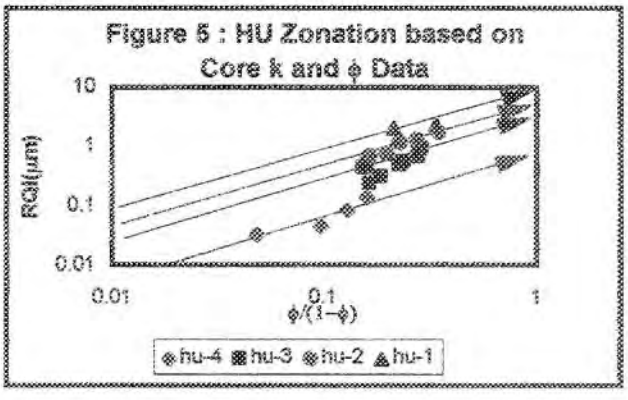
Figure 5 : HU Zonation based on Core k and ϕ Data
RQI(µm)
ϕ/(1−ϕ)
hu-4 hu-3 hu-2 hu-1

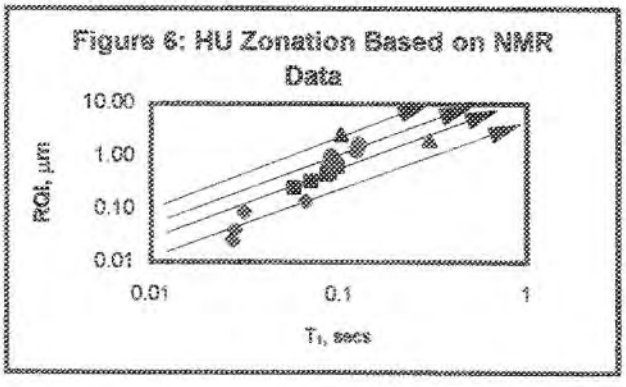
Figure 6: HU Zonation Based on NMR Data
RQI, µm
T1, secs

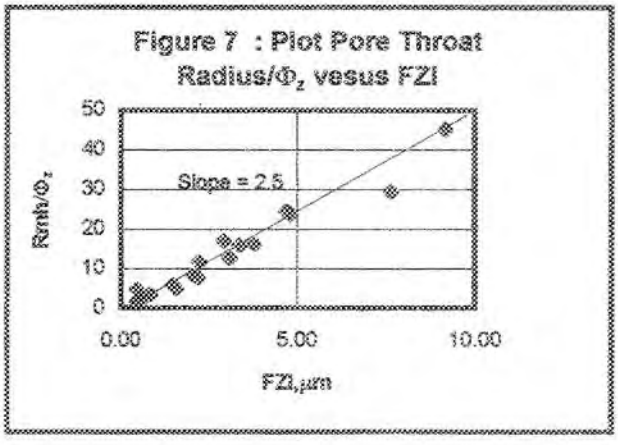
Figure 7 : Plot Pore Throat Radius/Φz vesus FZI
Rmh/Φz
Slope = 2.5
FZI,µm

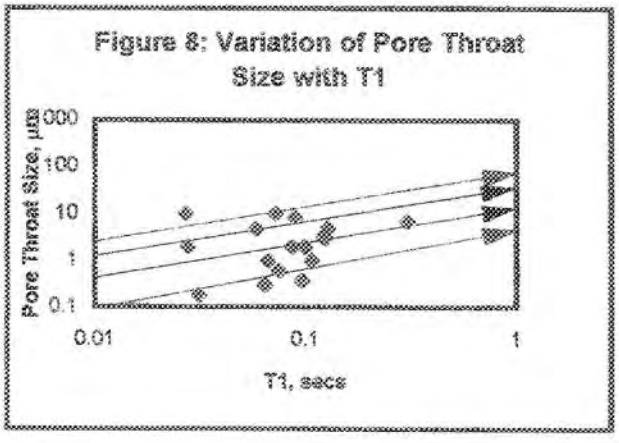
Figure 8: Variation of Pore Throat Size with T1
Pore Throat Size, µm
T1, secs

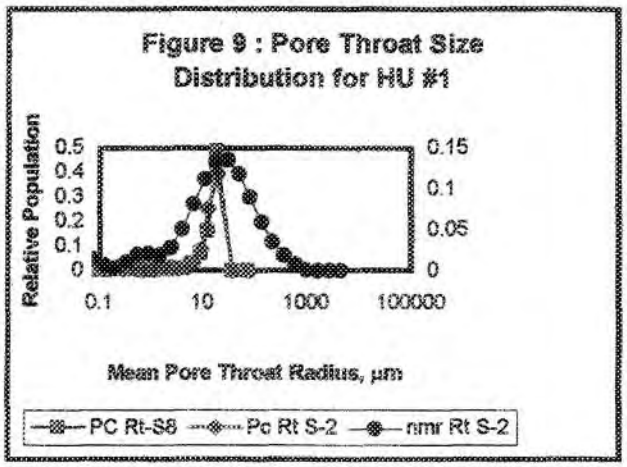
Figure 9 : Pore Throat Size Distribution for HU #1
Relative Population
0.5
0.4
0.3
0.2
0.1
0
0.15
0.1
0.05
0
0.1
10
1000
100000
Mean Pore Throat Radius, µm
PC Rt-S8
Pc Rt S-2
nmr Rt S-2

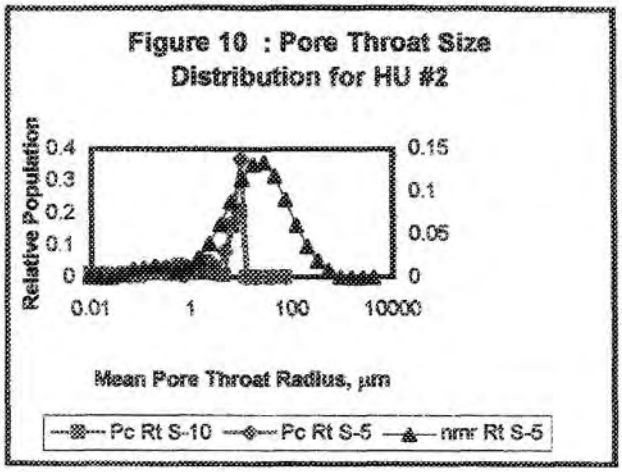
Figure 10 : Pore Throat Size Distribution for HU #2
Relative Population
0.4
0.3
0.2
0.1
0
0.15
0.1
0.05
0
0.01
1
100
10000
Mean Pore Throat Radius, µm
Pc Rt S-10
Pc Rt S-5
nmr Rt S-5

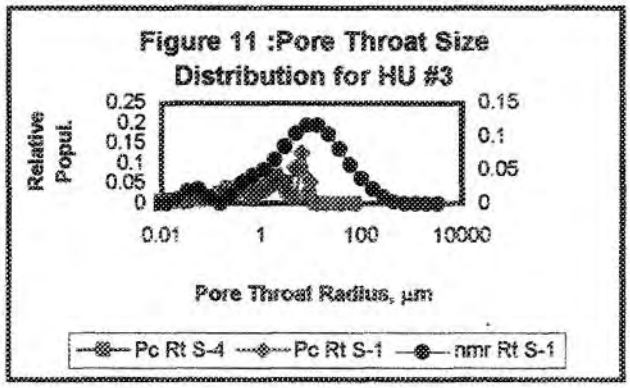
Figure 11 :Pore Throat Size Distribution for HU #3
Relative Popul.
0.25
0.2
0.15
0.1
0.05
0
0.15
0.1
0.05
0
0.01
1
100
10000
Pore Throat Radius, µm
Pc Rt S-4
Pc Rt S-1
nmr Rt S-1

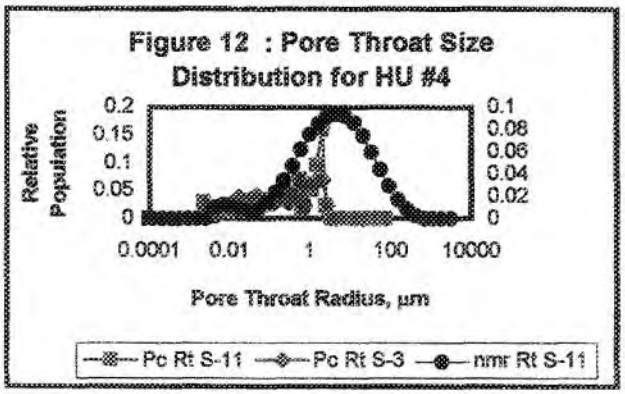
Figure 12 : Pore Throat Size Distribution for HU #4
Relative Population
0.2
0.15
0.1
0.05
0
0.1
0.08
0.06
0.04
0.02
0
0.0001
0.01
1
100
10000
Pore Throat Radius, µm
Pc Rt S-11
Pc Rt S-3
nmr Rt S-11

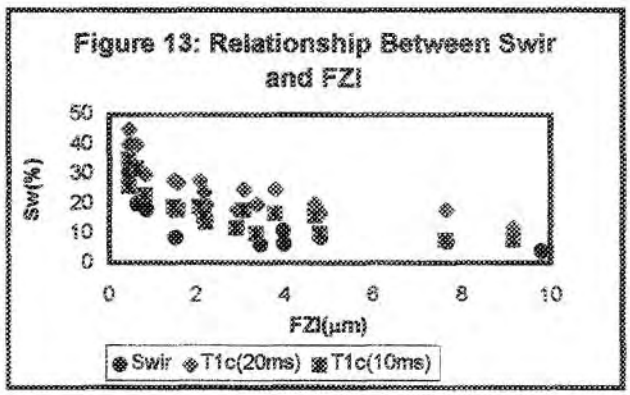
Figure 13: Relationship Between Swir and FZI
Sw(%)
50
40
30
20
10
0
0
2
4
6
8
10
FZI(µm)
Swir
T1c(20ms)
T1c(10ms)

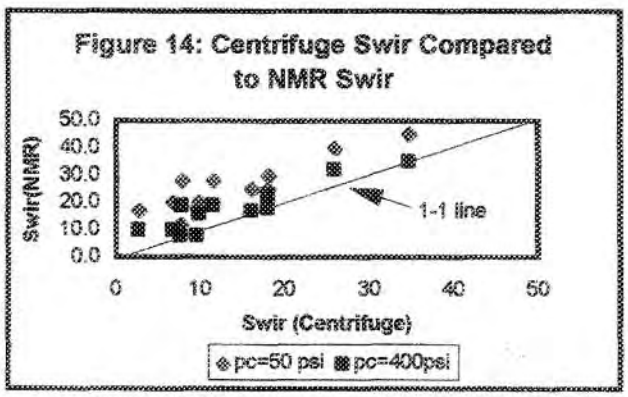
Figure 14: Centrifuge Swir Compared to NMR Swir
Swir(NMR)
50.0
40.0
30.0
20.0
10.0
0.0
1-1 line
0
10
20
30
40
50
Swir (Centrifuge)
pc=50 psi
pc=400psi

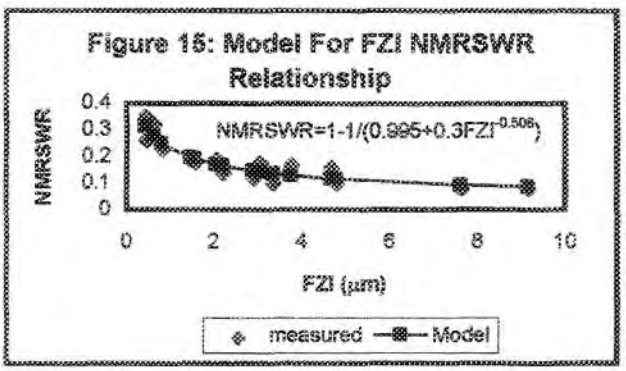
Figure 15: Model For FZI NMRSWR Relationship
NMRSWR
0.4
0.3
0.2
0.1
0
NMRSWR=1-1/(0.995+0.3FZI^0.508)
0
2
4
6
8
10
FZI (µm)
measured
Model

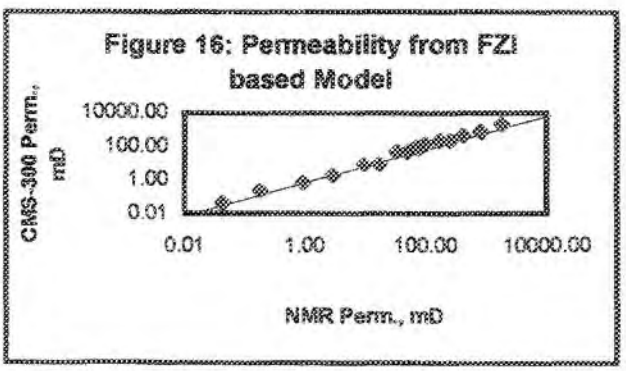
Figure 16: Permeability from FZI based Model
CMS-300 Perm., mD
10000.00
100.00
1.00
0.01
0.01
1.00
100.00
10000.00
NMR Perm., mD

1a : Pore Throat Size -Sample 1 HU 3

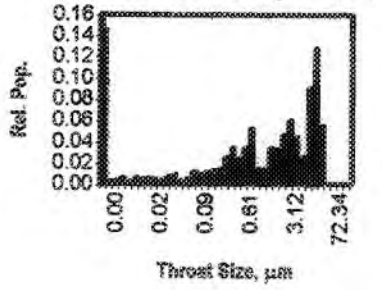

1b NMR Pore Size (Sample 1 HU 3)

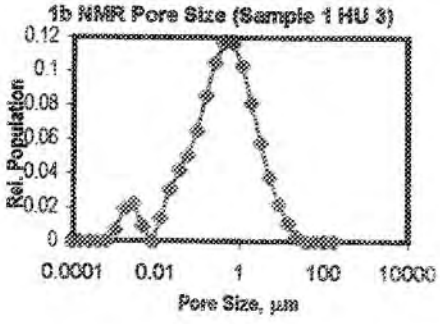

1c: Thin section(Sample 1 HU3)

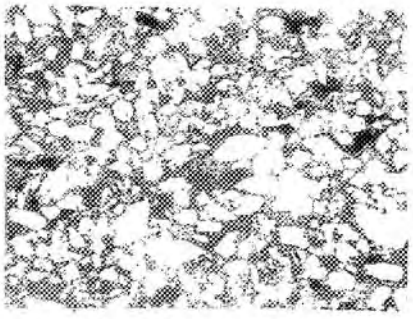

2a : Pore Throat Size -Sample 2 HU 1

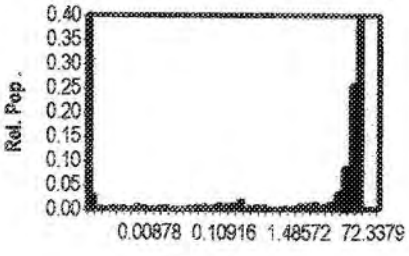

2b : NMR Pore Size -Sample2 HU 1

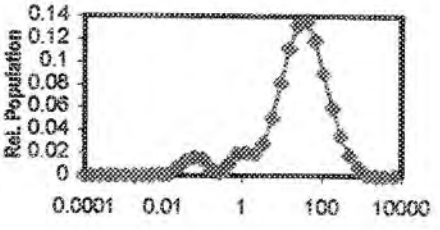

2c: Thin section(Sample 2 HU1)

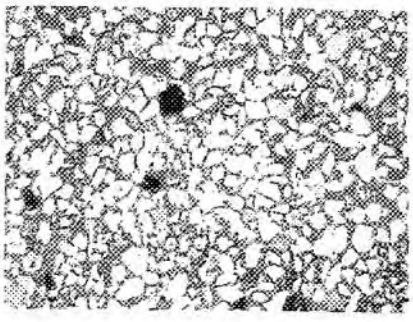

3a : Pore Throat Size-Sample 7 HU4

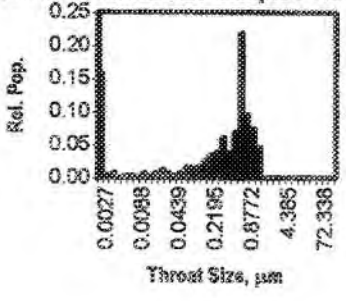

3b : NMRPore Size-Sample 7 HU 4

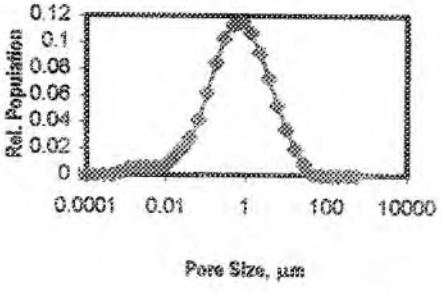

3c: Thin section(Sample 7 HU4)

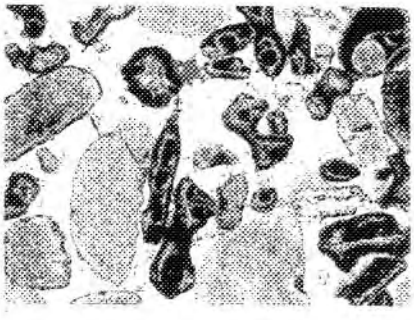

4a : Pore Throat Size-Sample 10 HU2

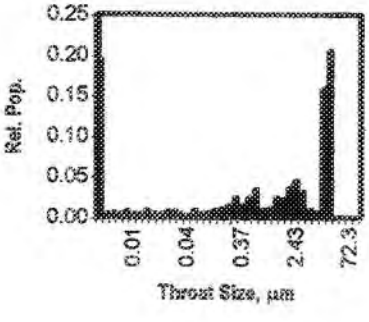

4b : NMR Pore Size-Sample 10- HU2

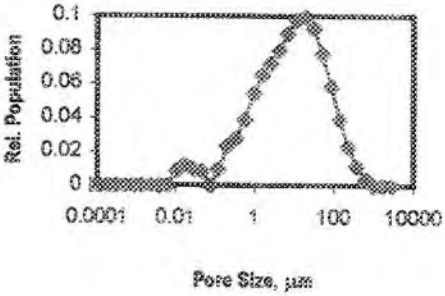

4c: Thin section(Sample 10 HU2)

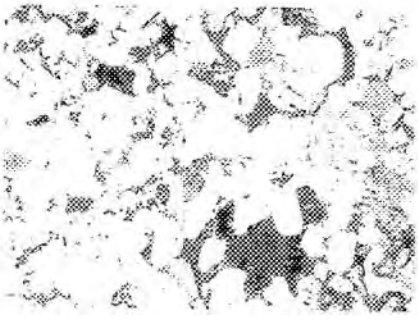

Figure 17: NMR Pore size, Mercury injectionThroat Size and Thin Section Images Comparison